https://ntrs.nasa.gov/search.jsp?R=19690023884 2020-03-12T05:00:31+00:00Z

N69-33262
NASA CR-86192

VAPOR PHASE GROWTH TECHNIQUE AND SYSTEM FOR SEVERAL III-V COMPOUND SEMICONDUCTORS

BY

J. J. TIETJEN, R. CLOUGH, A. B. DREEBEN, R. ENSTROM,
AND D. RICHMAN

INTERIM SCIENTIFIC REPORT NO. 2

MARCH 1969

Distribution of this report is provided in the interest of information exchange and should not be construed as endorsement by NASA of the material presented. Responsibility for the contents resides with the organization that prepared it.

PREPARED UNDER CONTRACT NO. NAS 12-538 BY

RCA LABORATORIES
PRINCETON, NEW JERSEY

ELECTRONICS RESEARCH CENTER
CAMBRIDGE, MASSACHUSETTS
NATIONAL AERONAUTICS AND SPACE ADMINISTRATION

Dr. James D. Childress
Technical Monitor
NAS 12-538
Electronics Research Center
575 Technology Square
Cambridge, Massachusetts 02139

Requests for copies of this report should be referred to:

NASA Scientific and Technical Information Facility
P. O. Box 33, College Park, Maryland 20740

VAPOR PHASE GROWTH TECHNIQUE AND SYSTEM FOR SEVERAL III-V COMPOUND SEMICONDUCTORS

BY

J. J. TIETJEN, R. CLOUGH, A. B. DREEBEN, R. ENSTROM,
AND D. RICHMAN

MARCH 1969

PREPARED UNDER CONTRACT NO. NAS 12-538 BY

RCA LABORATORIES
PRINCETON, NEW JERSEY

ELECTRONICS RESEARCH CENTER
CAMBRIDGE, MASSACHUSETTS
NATIONAL AERONAUTICS AND SPACE ADMINISTRATION

TABLE OF CONTENTS

Section		Page
SUMMARY	. . . .	1
I.	INTRODUCTION.	2
II.	TECHNICAL DISCUSSION.	2
	A. Growth of GaN and InN	2
	B. Growth of $In_{1-x}Ga_xP$ Alloys.	5
	C. Growth of $Ga_{1-x}Al_xAs$ Alloys	6
	D. Growth of $InAs_{1-x}P_x$ Alloys.	8
	E. Growth of GaSb and $GaAs_{1-x}Sb_x$ Alloys.	8
	F. Growth of InSb and $InAs_{1-x}Sb_x$ Alloys.	8
III.	CONCLUSIONS AND RECOMMENDATIONS	9
IV.	REFERENCES.	9
V.	NEW TECHNOLOGY APPENDIX	9
APPENDIX A	The Preparation and Properties of Vapor-Deposited Epitaxial $InAs_{1-x}P_x$ Using Arsine and Phosphine	10
APPENDIX B	Vapor-Phase Growth of Epitaxial $GaAs_{1-x}Sb_x$ Alloys Using Arsine and Stibine	18

LIST OF ILLUSTRATIONS

Figure | Page

A-1. Schematic representation of vapor-deposition apparatus. 11

A-2. The dependence of the alloy composition on the concentration of PH_3 in the AsH_3-PH_3 gas mixture 12

A-3. The dependence of the lattice constant on alloy composition in the system $InAs_{1-x}P_x$. The dependence observed by Folberth (Ref. A-1) and Koster and Ulrich (Ref. A-14) is also included: --- Folberth; —— — —— Koster and Ulrich; —— this report . . . 14

A-4. The dependence of the electron mobility on alloy composition in the system $InAs_{1-x}P_x$ at room temperature. The experimental results of Weiss (Ref. A-2) and a theoretical analysis of Ehrenreich (Ref. A-15) are also included: --- Weiss; —— Ehrenreich; • this report. 15

A-5. The dependence of the electron mobility on alloy composition in the system $InAs_{1-x}P_x$ at 77°K. 15

B-1. Schematic representation of the vapor-deposition apparatus. . . . 19

B-2. Schematic representation of the stibine storage and sampling apparatus 21

LIST OF TABLES

Table | Page

I. Electrical Properties of Undoped GaN. 4

II. Electrical Properties of GaN Doped with Acceptor Impurities . . . 4

III. Representative Growth Rates of GaAs and $Ga_{1-x}Al_xAs$ Alloys 7

B-1. Electrical Properties of P-type $GaAs_{1-x}Sb_x$ Alloys 22

B-2. Electrical Properties of N-type $GaAs_{1-x}Sb_x$ Alloys 23

VAPOR-PHASE GROWTH TECHNIQUE AND SYSTEM FOR SEVERAL III-V COMPOUND SEMICONDUCTORS

by

J. J. Tietjen, R. Clough, A. B. Dreeben, R. E. Enstrom, and D. Richman

RCA Laboratories
Princeton, New Jersey

SUMMARY

Significant progress has been made during the past year in extending the vapor-phase growth method to the preparation of III-V compounds containing Al and nitrogen, on the completion of the growth of the antimonides, and on the growth and characterization of $In_{1-x}Ga_xP$ alloys. As a result, most of the contract objectives of the first two years have been met, demonstrating the versatility and compatibility of the ERC vapor-phase growth system.

For the first time single-crystalline, colorless layers of GaN have been grown with sufficient size to permit good electrical and optical characterization of this material. Good control of the composition of $In_{1-x}Ga_xP$ alloys has been achieved, and it has been determined that these alloys have direct band gaps as large as 2.12 eV. These alloys have been doped both n- and p-type, and orange electroluminescence has been generated by an $In_{1-x}Ga_xP$ p-n junction.

$GaAs_{1-x}Sb_x$ alloys have been prepared across the entire alloy series with good control of the composition. For the first time donor impurities have been added to GaSb during vapor-phase growth, and this has permitted the preparation of vapor-grown p-n junction structures. A p-type alloy with 4% GaSb was prepared with a mobility of 400 cm^2/V-sec, which is equivalent to the highest yet reported for unalloyed p-type GaAs. $Ga_{1-x}Al_xAs$ alloys have been prepared as single-crystalline layers which is the first time that this material has been prepared from the vapor phase. Polycrystalline InSb and $InAs_{1-x}Sb_x$ alloys, with $x > 0.95$ have been prepared.

I. INTRODUCTION

During the first year of this contract, the primary objective was to develop a compatible vapor-phase growth method for the preparation of GaAs, GaP, GaSb, InAs, InP, InSb, and selected alloys of these compounds. Further, the method was to have the capability of providing both n- and p-type doping and the preparation of multilayer structures. To accomplish these objectives the RCA method of vapor growth, used previously with great success for the preparation of GaAs and $GaAs_{1-x}P_x$ alloys, was chosen and was modified to permit the preparation of compounds containing In and Sb.

In this way, all of the above compounds, except InSb, were prepared as single crystals. In addition, alloys of $GaAs_{1-x}P_x$, $InAs_{1-x}P_x$, $GaAs_{1-x}Sb_x$, $In_{1-x}Ga_xAs$, and $In_{1-x}Ga_xP$ were also grown as pure, single-crystalline epitaxial layers. Also, p- and n-type doping and the preparation of multilayer structures in selected materials was achieved, which demonstrated the ability of this vapor-phase method to fulfill the objectives of the program.

In order to extend the utility of this vapor growth system, work during the second year focussed on the preparation of III-V compounds containing Al and nitrogen by the addition of Al and NH_3 sources. Also, the antimonide work has been completed, and the growth and characterization of $In_{1-x}Ga_xP$ alloys has been continued because of its potential for visible electroluminescence. Again the method has demonstrated its ability to meet the program objectives, even though several of these goals are exceptionally difficult to attain because of problems related to the instability of SbH_3 at room temperature and the corrosiveness of the aluminum chlorides.

II. TECHNICAL DISCUSSION

A. Growth of GaN and InN

GaN has been vapor-grown using equipment and gas flow rates similar to that used for GaAs except that NH_3 is used in place of AsH_3 and, in initial experiments, a N_2 carrier gas was used instead of Pd-diffused H_2. After about 20 runs, the thermal conditions, flow rates, and gas concentrations were determined sufficiently well so that polycrystalline GaN could be deposited on a vitreous quartz substrate at 750°C. Subsequent experiments to achieve single-crystalline GaN layers focussed on the effect of substrate and temperature. The use of a wide variety of single-crystalline substrates or of a range of deposition temperatures was ineffective in promoting the growth of single-crystalline GaN layers. However, it was demonstrated that GaN could be grown at temperatures as low as 550°C; but even at this low temperature, significant oxygen contamination was present to color the crystal yellow.

The problem of oxygen contamination was overcome by using high-purity NH_3, which then permitted high-purity Pd-diffused H_2 to be used in place of the N_2 carrier gas. This then led, after about 40 runs to optimize growth conditions, to the growth at 825°C of single-crystalline, colorless layers of GaN on <0001> oriented sapphire at a growth rate of about 1/2 micron/min. Thus, for the first time, single-crystalline layers of GaN are available of sufficient size to allow good measurements of the optical and electrical properties to be made.

These layers are single-phase, hexagonal GaN with the wurtzite structure and have lattice parameters a = 3.189 Å and c = 5.185 Å. Optical absorption measurements on undoped GaN revealed a very sharp absorption edge at 3.39 eV, and analysis of absorption vs. wavelength relationship indicates that the energy gap is direct. The reflectivity of polished GaN is 30% over the range 4000 to 6000 Å.

The results of Hall-effect measurements for several undoped GaN samples are shown in Table I. Since the total impurity concentration, as determined by mass spectrometric analysis, is less than 10 ppm, the high carrier concentrations are attributed to a native defect, such as nitrogen vacancies(Ref.1).

In an effort to achieve high-conductivity p-type GaN, the layers were doped during growth with Zn, Hg, Mg, and Si. Zn-doping produces orange-colored, high-resistivity, p-type GaN, indicating that the Zn forms a deep acceptor level(Ref.2). It was possible to make electrical measurements on two lightly Zn-doped samples and the results are shown in Table II. Here it may be seen that the samples are n-type and that the net electron concentration is less than observed for undoped GaN, Table I, indicating the occurrence of some compensation. For sample 12•23•68•M, there is also a marked increase in mobility, even though chemical analysis shows a Zn concentration of $1x10^{20}$ cm^{-3}. The high observed mobility of the sample most likely results from a reaction of the zinc with the donor, to produce a complex having a lower charge state and a smaller scattering cross section.

GaN samples doped with Hg were all highly conducting n-type, suggesting that the solubility of Hg in GaN is relatively low at the 825°C growth temperature.

Mg doping of GaN leads principally to yellow, high-resistivity layers which indicates that Mg, like Zn, is probably a deep-level acceptor. One Mg-doped sample appeared to be highly conducting p-type from resistivity and thermal probe measurements. However, these layers were not uniformly doped and exhibited some n-type conductivity regions. To date, efforts to increase the Mg concentration either have prevented the growth of single-crystalline GaN or have resulted in n-type layers.

Doping GaN with Si, which could substitute for either Ga or N, does not lead to high-conductivity p-type layers either, but does appear to lower the electron concentration by compensation as shown in Table II. For sample 2•24•69•M, this compensation is quite close since the electron concentration has been reduced to $3x10^{16}$ cm^{-3}.

TABLE I

ELECTRICAL PROPERTIES OF UNDOPED GaN

Sample	n, (cm^{-3})	ρ, (Ω-cm)	μ, (cm^2/V-sec)
11•22•68:M	6.7×10^{19}	.0080	12
12•6•68:M	3.0×10^{19}	.0062	32
1•28•69:M2	4.5×10^{19}	.0030	47

TABLE II

ELECTRICAL PROPERTIES OF GaN DOPED WITH ACCEPTOR IMPURITIES

Sample	Dopant	n, (cm^{-3})	ρ, (Ω-cm)	μ, (cm^2/V-sec)
11•29•68:M2	Zn	8.8×10^{18}	0.134	67
12•23•68:M	Zn	3.0×10^{18}	0.0042	500
2•24•69:M	Si	3.0×10^{16}	18.3	11
3•6•69:M	Si	2.0×10^{19}	0.0038	85

A preliminary study of the growth of InN was initiated, also using NH_3 as the source of nitrogen. To date, little information has been reported for this compound because it is very difficult to prepare, especially from the vapor phase. InN dissociates at temperatures above about 500°C and thus very low growth temperatures (< 500°C) must be used. However, at such low temperatures, the vapor pressure of InCl is very low, so that it tends to condense if present in the concentrations required to achieve a reasonable growth rate of InN. Therefore, oxide transport of In was investigated in a series of five runs using high-purity oxygen gas as the transport agent. X-ray analysis confirmed that InN had been successfully deposited as a polycrystalline film on vitreous quartz substrates at about 500°C. However, further examination showed the deposit to be a two-phase mixture of In and InN. In view of the difficulties associated with the vapor growth of InN and the high dissociation pressure which limits practical application of the material, it is anticipated that no further attempts will be made to improve the purity and crystallinity over that achieved already.

B. Growth of $In_{1-x}Ga_xP$ Alloys

The work on the vapor growth of $In_{1-x}Ga_xP$ alloys for the past year has been directed toward obtaining material with a direct band gap greater than that found in the $GaAs_{1-x}P_x$ system, in an effort to obtain material having potential for efficient visible electroluminescence. In the course of this work several difficulties have been encountered and to a large extent overcome.

First it was found that indium-rich alloys were not easily prepared. This is related to the greater relative stability of indium monochloride compared with gallium monochloride and to the higher dissociation pressure of InP relative to GaP, under the experimental conditions used. By modifying the gas flow conditions and by increasing the concentration of phosphine in the gas phase it was possible to overcome this difficulty.

A second major problem is that of strain in the grown layers. This has two causes: the mismatch in lattice constant between the alloy and the substrate and the difference in their thermal expansion coefficients. The lattice mismatch can be minimized by growing alloys near the composition $In_{.43}Ga_{.57}P$ since for this composition the alloy lattice constant matches that of the GaAs substrate. The thermal-expansion strain, however, has not been overcome. This composition range around 50% InP is a good one for investigating the electroluminescent behavior of this alloy system. Hence, the band gap is about 2.0 eV and is direct; but it is well removed from the crossover to an indirect transition both in composition and energy. The crossover point is at 2.2 eV and has a composition of $In_{.24}Ga_{.76}P$.

Throughout most of the work to this point only n-type material was grown, and junctions were formed by zinc diffusion. In many but not all cases, light-emitting junctions were obtained. Although orange, band-edge emission was obtained the luminescence was dominated by weak low-energy emison and the maximum room-temperature efficiencies were only about 10^{-4} percent.

Recently we have begun to grow junctions by vapor deposition. At first a p-type alloy was grown on top of an n-type layer. However, in all cases the zinc diffused through the alloy n-layer and into the GaAs substrate so that the junctions emitted infrared rather than visible light. To avoid this problem, the growth order was reversed. Starting with a p-type GaAs substrate, a p-type alloy layer was grown first and the n-type layer was grown last. This technique yielded sharp, flat junctions in the $In_{1-x}Ga_xP$ alloy but the as-grown junctions did not emit visible light. However, it was found that annealing the p-n junction structure for 4 hours at 800°C is effective in promoting visible electroluminescence. The reason for this is presently under investigation. Recent Hall-effect measurements on separate layers suggest that the p- and n-type doping concentrations may be too high and, therefore, work at the present time is directed toward optimizing the doping levels.

C. Growth of $Ga_{1-x}Al_xAs$ Alloys

The work on preparing $Ga_{1-x}Al_xAs$ alloys has concentrated on preparing alloys containing from 10 to 40 mole percent AlAs because materials in this range are of interest for electroluminescence and also avoid the problem of hygroscopicity associated with AlAs-rich alloys.

Initial efforts to achieve single-crystal alloy layers were not successful. Attack of the quartz growth tube by AlCl and the resultant oxygen contamination (as silicates or oxides) was suspected as a possible cause of the polycrystalline layers. Coating the quartz growth tube with carbon prevented attack by the AlCl but did not promote single-crystalline deposits. Next, about 30 runs were made to determine the effect of other growth parameters on the crystallinity. It was found that approximately 50% lower total H_2 carrier gas flow rates are required to prepare single-crystalline unalloyed GaAs, as well as the alloy layers, when the higher temperatures needed for the efficient transport of aluminum (e.g., aluminum source and reaction zone temperatures greater than 1000°C) are used.

Another series of runs was made to determine growth rates of GaAs and $Ga_{1-x}Al_xAs$ alloys for various combinations of gas flow rates. Some representative values determined by metallographic examination of cleaved and stained surfaces are given in Table III. Here it is interesting to note that relatively high GaAs growth rates can be attained with low HCl flow rates over the Ga source, and that the alloy growth rate is generally less than for unalloyed GaAs. Spectrographic and optical absorption analysis of some single-crystalline layers from which the substrates had been removed by chemical polishing show that up to 3 mole percent AlAs has been incorporated. Recently, another layer with single-crystalline areas (#13, Table III) was prepared with colors ranging from yellow to orange-red indicating the presence of substantial amounts of AlAs. However, the color range indicates that the AlAs is inhomogeneously distributed throughout the wafer. From optical absorption data, the AlAs content is estimated to range from 10 to 30 mole percent, with the maximum possibly extending to 60 mole percent. The main problem now is to control the growth conditions so that homogeneous, single-crystalline layers with the required AlAs concentration can be prepared consistently.

TABLE III

REPRESENTATIVE GROWTH RATES OF GaAs AND $Ga_{1-x}Al_xAs$ ALLOYS

	Flow Rate - cm^3/min				Growth Rate-μ/hr	
	HCl/H_2 Over Ga	HCl/H_2 Over Al	10% AsH_3 in H_2	Carrier H_2	GaAs	Alloy
1	5/400	0/400	150	1100	14	-
2	5/200	0/600	150	700	36	-
3	5/200	1/600	150	700	-	29
4	5/200	5/600	300	700	-	20
5	5/200	5/600	50	700	-	9
6	5/400	0/400	150	700	44	-
7	1/400	0/400	150	700	37	-
8	1/400	5/400	150	700	-	23
9	1/400	5/400	200	700	-	15
10	0.2/400	0/400	150	700	16	-
11	0.2/400	1/400	150	700	-	2
12	0.53/400	0/400	150	700	22	-
13	0.53/400	1/400	150	700	-	4

D. Growth of $InAs_{1-x}P_x$ Alloys

A paper describing in detail the preparation and electrical properties of $InAs_{1-x}P_x$ alloys, grown primarily during the first year of this contract, is attached as Appendix A. Single-crystalline $InAs_{1-x}P_x$ alloy layers were prepared with the highest electron mobilities yet reported for this system. At 77°K, a mobility value of 120,000 cm^2/V-sec was measured for InAs which exceeds any previously reported. Both n- and p-type doping have been achieved during vapor growth to provide a broad range of electrical resistivities and p-n junctions.

E. Growth of GaSb and $GaAs_{1-x}Sb_x$ Alloys

A complete description of the preparation and properties of GaSb and $GaAs_{1-x}Sb$ alloys is given in a paper that has been submitted for publication and is included in the present report as Appendix B. In summary, it has been found that single-crystal GaSb and $GaAs_{1-x}Sb_x$ alloys across the entire alloy series could be grown from the vapor phase using stibine as the source of antimony. This is the first time that the alloy series has been grown from the vapor phase. To accomplish this, special handling techniques had to be developed for using the stibine, which must be stored at -78° to prevent decomposition. Layers of p-type GaSb and GaSb-rich alloys have been grown with carrier concentrations comparable to the lowest ever reported. In addition, a mobility of 400 cm^2/V-sec has been measured in a p-type alloy containing 4% GaSb, which is equivalent to the highest reported for p-type GaAs. Strain and inhomogeneity appear to limit the electrical properties of alloys with higher GaSb concentrations.

Undoped GaSb is always p-type. Therefore, the addition of Te and Se donor impurities during vapor growth of GaSb was investigated to achieve n-type doping and p-n junctions. It was found that Te provides n-type conductivity more readily than Se, probably because the solubility of Te in GaSb is higher. However, the rapid diffusion of Te in GaSb requires low growth temperatures to prevent the dopant from diffusing out of the growing layer and into the substrate. By using deposition temperatures as low as 400°C, it has been possible to prepare Te-doped GaSb with net electron concentrations as high as 2×10^{17} cm^{-3}. Consequently, for the first time, p-n junction structures have been prepared in GaSb by vapor-phase growth.

F. Growth of InSb and $InAs_{1-x}Sb$ Alloys

The vapor-phase growth of InSb was initiated using stibine as the source of Sb. The preparation of this compound is one of the most difficult problems in this contract, since the combined low melting point of InSb and the low vapor pressure of Sb impose growth conditions which severely limit the surface mobility of the reactant species, and favor the formation of metallic Sb as a second phase. In addition, the proper growth conditions must necessarily result in low growth rates. To accommodate these difficulties, very dilute concentrations of SbH_3, and growth temperatures as near the melting point of the compound as possible, were used to prepare several layers of InSb and $InAs_{1-x}Sb_x$ for $x > 0.95$. In all cases, however, these layers were

polycrystalline and no electrical measurements were made. Because of these inherent difficulties, and since other phases of this research appear to be more important, the work on this system is being discontinued.

III. CONCLUSIONS AND RECOMMENDATIONS

Most of the objectives of the contract extension have been successfully accomplished during the past year. The versatility of the ERC growth system has again been demonstrated with the preparation of III-V compounds containing aluminum, nitrogen, and antimony. Thus, GaN, InN, GaSb, InSb, and the alloys of $GaAs_{1-x}Sb_x$, $InAs_{1-x}Sb_x$, and $Ga_{1-x}Al_xAs$ have been added to the substantial number of materials prepared during the first year by this vapor-growth method. With several of these materials single-crystalline n- and p-type layers, and multi-layer structures have been prepared for the first time by vapor-phase growth.

In accordance with the objectives of the contract extension, work will be initiated on the extension of the ERC vapor-growth system to the preparation of single crystalline layers of the compounds AlN, AlP, AlAs, and AlSb. In addition, studies will continue on the doping of GaN with acceptor impurities, the preparation of $In_{1-x}Ga_xP$ alloy p-n junction layers for electroluminescent applications, and the growth of $Ga_{1-x}Al_xAs$ alloys. Also, preparation of $Ga_{1-x}In_xN$ alloys will be attempted.

IV. REFERENCES

1. A. Rabenau in Compound Semiconductors, Vol. 1, edited by R. K. Willardson and H. L. Goering, (Reinhold Book Corp., New York, 1962).

2. H. G. Grimmeiss, R. Groth, and J. Maak, Z. Naturforsch. 15a, 799 (1960).

V. NEW TECHNOLOGY APPENDIX

Title: Visible Light Electroluminescent Diodes of $In_{1-x}Ga_xP$.

Page reference: 5,6

Comments: P-N junction electroluminescent diodes that emit orange light have been prepared both by vapor growth and by acceptor impurity diffusion in $In_{1-x}Ga_xP$ alloys.

APPENDIX A

The Preparation and Properties of Vapor-Deposited Epitaxial $InAs_{1-x}P_x$ Using Arsine and Phosphine

by

J. J. Tietjen, H. P. Maruska, and R. B. Clough
RCA Laboratories, Princeton, N. J. 08540

ABSTRACT

Single-crystalline $InAs_{1-x}P_x$ layers have been prepared by a vapor-phase growth technique previously used to prepare very high-quality $GaAs_{1-x}P_x$. These $InAs_{1-x}P_x$ alloys exhibit the highest electron mobilities yet reported for this system. Electron mobility data are reported for the alloys at 77°K for the first time. At this temperature, a mobility value of 120,000 cm^2/V-sec was measured for InAs, which is the highest yet reported. Vegard's law is obeyed over the entire composition range. Both n- and p-type doping have been achieved during vapor growth to provide a broad range of electrical resistivities and p-n junctions.

I. Introduction

$InAs_{1-x}P_x$ alloys have an exceptionally broad range of band gaps and electron mobilities. Consequently, they have potential advantage for a number of device applications. These include infrared emitting and detecting devices, utilizing their low energy band gaps, and devices operating at high frequencies, which can take advantage of their high mobilities. Nevertheless, only limited results (Refs. A-1 - A-3) have been reported pertaining to improving the preparation and properties of these crystals, and virtually no work has involved the vapor-phase growth of these materials. As a result, the potential of $InAs_{1-x}P_x$ alloys has not been fully realized.

In contrast, with $GaAs_{1-x}P_x$ alloys, a very significant effort has been undertaken to improve and characterize these materials, and in this respect, vapor-phase growth methods have played a significant role (Refs. A-4 - A-8). In particular, one vapor-phase growth technique (Ref. A-8) has been developed which permits the preparation of $GaAs_{1-x}P_x$ alloys with high purity, homogeneity, and crystalline perfection. In addition, this method facilitates controlled n- and p-type doping over a wide resistivity range, and the preparation of multilayer structures incorporating layers of different resistivity and/or composition. This, in turn, has led to the fabrication of a variety of outstanding electro-optic (Refs. A-9 - A-11) and microwave (Refs. A-12 - A-13) devices. With this growth method, Ga is transported as its subchloride via a reaction with HCl gas, and AsH_3 and PH_3 serve as the sources of the group V elements.

As a logical extension of this growth technique, a simple substitution of In for the Ga has permitted the preparation of $InAs_{1-x}P_x$ single crystals having the highest electron mobilities ever reported, which supplements the earlier work on $GaAs_{1-x}P_x$. In addition, both n- and p-type doping has been achieved, and multilayer structures have been prepared.

II. Experimental

A. Apparatus and Materials. -- The apparatus, shown schematically in Figure A-1, is essentially identical to that described previously (Ref. A-8) with the

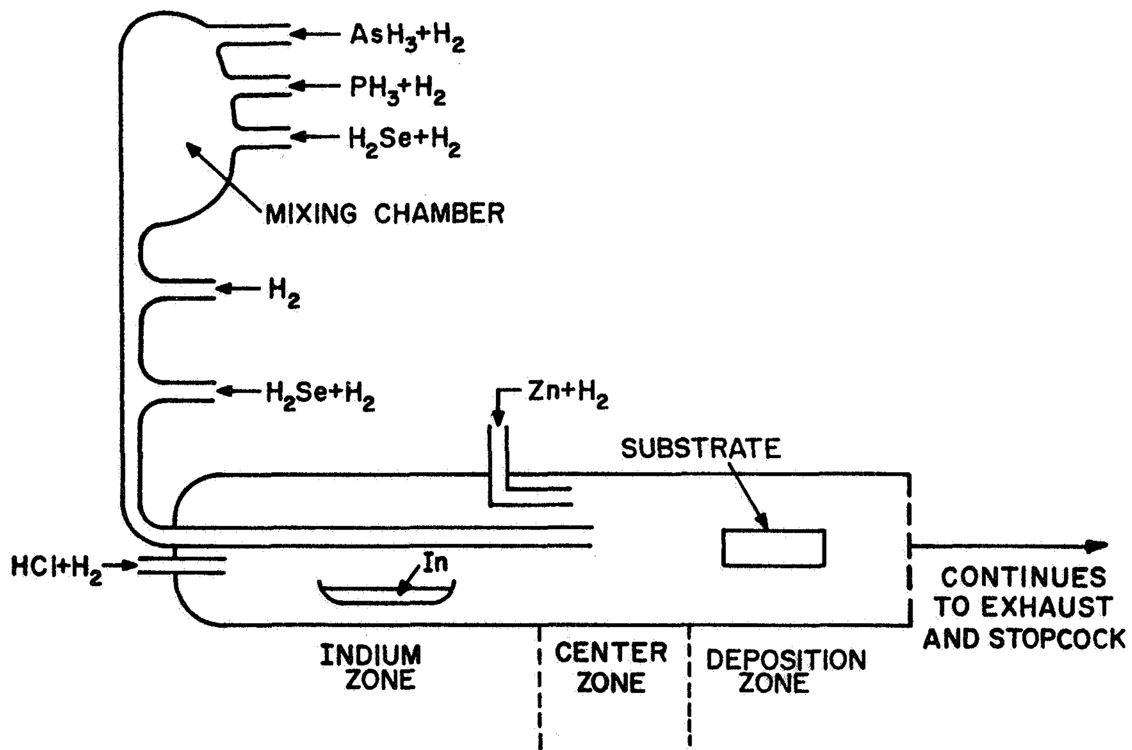

Figure A-1. Schematic representation of vapor-deposition apparatus.

exception that the source Ga is replaced by In. It consists principally of a straight tube through which the pertinent vapors pass. A large bore stopcock separates the growth region from a forechamber which may be independently purged to facilitate insertion and withdrawal of the specimens without contaminating the system. HCl gas, AsH_3, PH_3, and H_2Se, which serves as the n-type dopant source, are all monitored into the apparatus by precision valves and flowmeters. P-type doping is achieved by vaporizing metallic Zn in a heated side-arm and transporting the vapors into the deposition zone with H_2 carrier gas.

With the exception of the use of <100>-oriented InAs single-crystalline substrates,* the materials employed in this study are as described previously (Ref. A-8). The InAs substrates were mechanically polished to a flat, mirror-smooth finish, and then chemically polished in a solution of 2% by volume of bromine in methanol. Typical substrate dimensions were about 2 cm^2 in area and 0.5 mm thick.

B. Procedure. -- The growth procedure also closely follows that described previously (Ref. A-8). Freshly etched substrates are inserted in the growth chamber and heated in hydrogen at a rate of about 20°C/min. When the substrate temperature reaches 600°C, the AsH_3 flow is started in order to provide an arsenic atmosphere to stabilize the substrate surface. When the final operating temperatures are reached, the HCl flow over the In is started and the epitaxial deposition of InAs occurs. The flow of PH_3 is then initiated and slowly increased to produce a final gas phase mixture of AsH_3 and PH_3 appropriate to the desired alloy composition. The dependence of the alloy composition on the concentration of PH_3 in the AsH_3-PH_3 mixture is presented in Figure A-2.

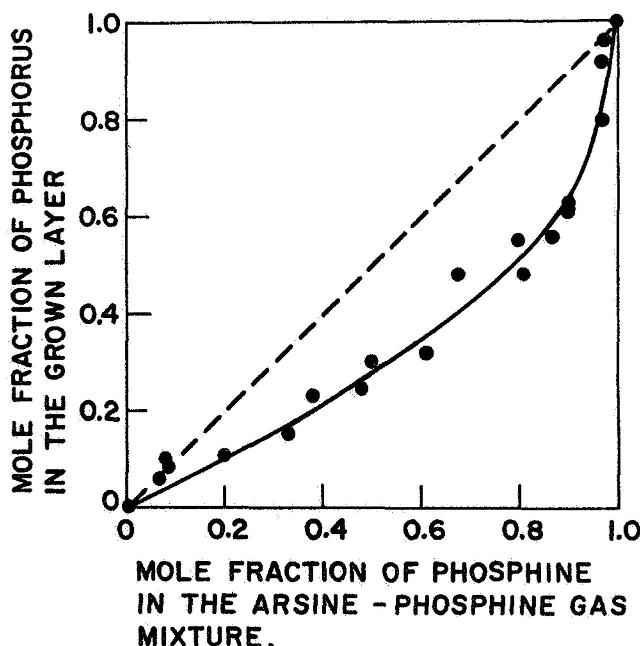

Figure A-2. The dependence of the alloy composition on the concentration of PH_3 in the AsH_3-PH_3 gas mixture.

* Purchased from Monsanto Company, St. Louis, Missouri.

By slowly increasing the PH_3 flow, a region is introduced which is graded in composiition from InAs at the substrate to the selected alloy composition. This graded region, which has been as thick as 50 microns for phosphorus-rich alloys, is included to minimize strain arising from differences between the lattice constants of the substrate and the final alloy layer.

The sum of the flow rates of pure AsH_3 and PH_3 is in the range of 20 to 60 cc/min. The HCl flow rate is about 5 cc/min, and between 1 and 2 l/min of hydrogen is used as a carrier. With these flow rates, with a substrate temperature in the range of 675 to 725°C, a center zone temperature of 950 to 975°C, and an indium zone temperature of between 850 to 950°C, growth rates in the range of 1/4 to 1/2 micron/min are obtained under steady-state conditions. Typical thicknesses for the constant composition region of these deposits have been between 50 and 150 microns.

III. Results and Discussion

A. Crystallinity and Growth Morphology. -- X-ray analysis by the Debye-Scherrer technique indicates that these layers are single phase, cubic, solid solutions, and show no detectable range of composition. In addition, Laue back-reflection analysis reveals that the layers are epitaxial. The lattice constant is presented as a function of alloy composition in Figure A-3, which demonstrates that Vegard's law of solid solutions is obeyed in this system. This result is in general agreement with those of Folberth (Ref. A-1), and Koster and Ulrich (Ref. A-14). The compositions were determined by chemical analysis (Ref. A-15) with an accuracy of $\pm$ 0.5%.

Although no detailed evaluation of the crystalline perfection of these layers was carried out, examination by optical microscopy revealed that microscopic surface imperfections, such as hillocks, were prevalent only in phosphorus-rich alloys. For alloys containing less than 50% InP, surfaces are obtained which show virtually no gross structure, and to the unaided eye appear to be mirror-smooth.

B. Electrical Properties. -- The epitaxial layers were examined by Hall coefficient and resistivity measurements using a technique (Ref. A-8) which permits these measurements to be made on layers as thin as 50 microns. Typical electron carrier concentrations for undoped alloys are in the range of $5x10^{15}$ to $1x10^{16}/cm^3$. The electron mobilities are presented as a function of alloy composition in Figures A-4 and A-5 for room temperature and 77°K, respectively. The data of Weiss (Ref. A-2) and the results of a theoretical analysis of Ehrenreich (Ref. A-16) based on the absence of alloy scattering in this system, and assuming perfect purity, are included for comparison. In general, the mobility values at room temperature are very high, with several values exceeding the best previously reported. In addition, these data corroborate Ehrenreich's contention that alloy scattering is negligible in this alloy system, at room temperature. The relatively low values obtained for alloy compositions approaching InP are attributed to strain arising from lattice and thermal-expansion differences between the InAs substrate and the

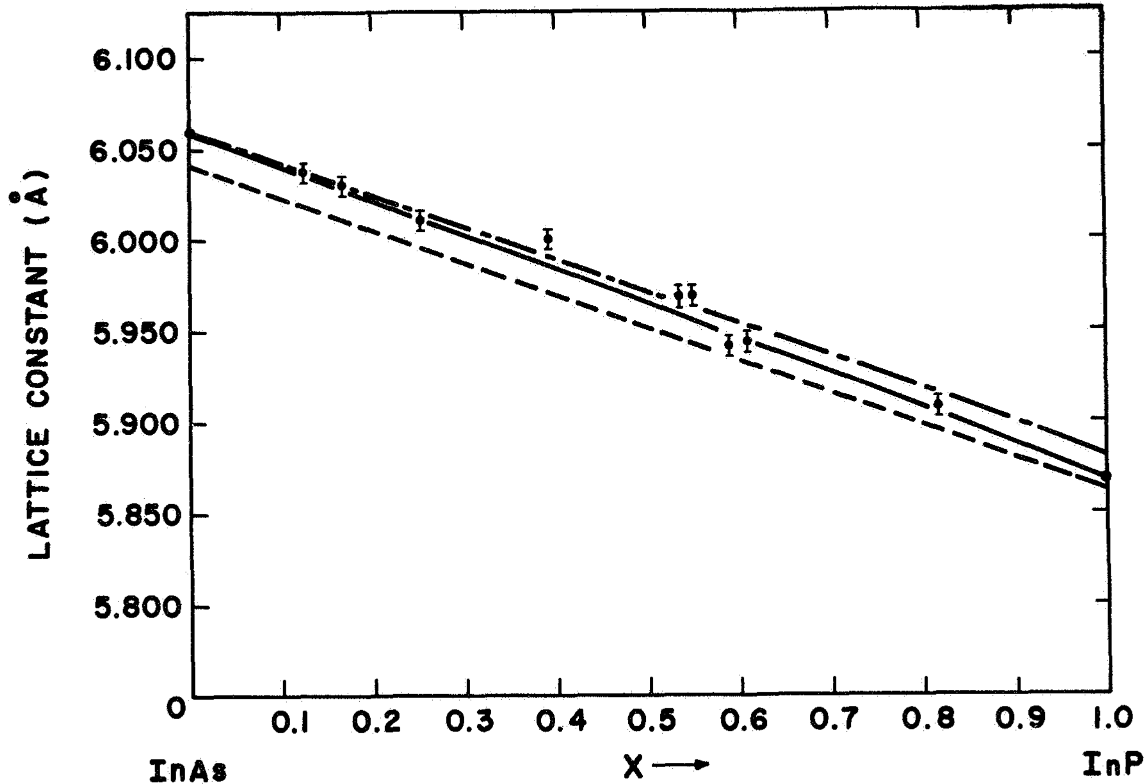

Figure A-3. The dependence of the lattice constant on alloy composition in the system $InAs_{1-x}P_x$. The dependence observed by Folberth (Ref. A-1) and Koster and Ulrich (Ref. A-14) is also included: --- Folberth; —— – —— Koster and Ulrich; ——— this report.

alloy layer. It is anticipated that further compositional grading can alleviate this problem.

The data presented in Figure A-5 are the first ever reported for 77°K for this alloy system. These high values indicate that the crystals are nearly uncompensated. It is particularly noteworthy that the value of 120,000 cm^2/V-sec for InAs is the highest ever reported for 77°K (Ref. A-17).

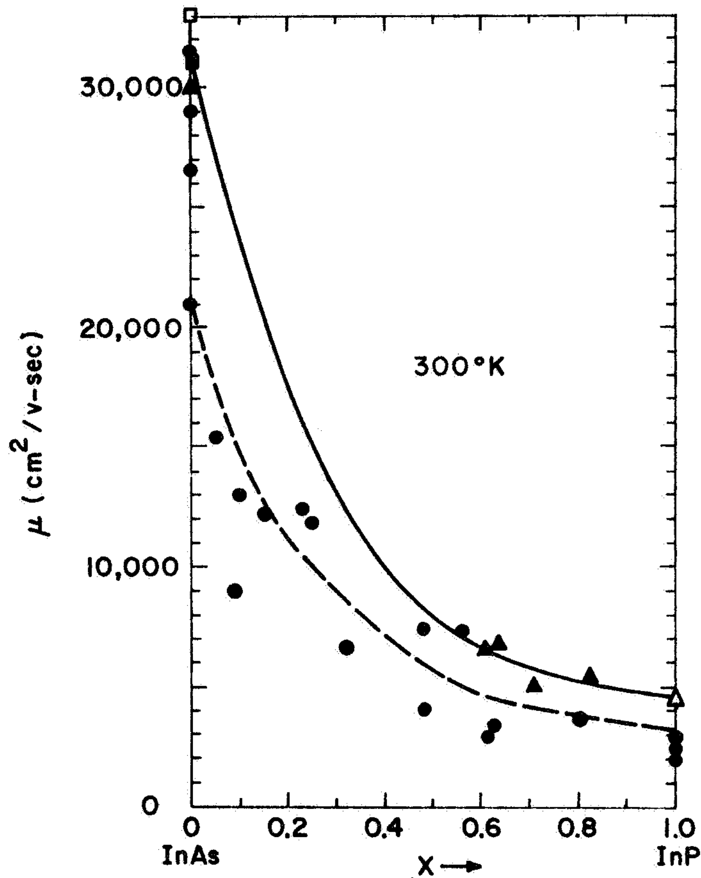

Figure A-4.

The dependence of the electron mobility on alloy composition in the system $InAs_{1-x}P_x$ at room temperature. The experimental results of Weiss (Ref. A-2) and a theoretical analysis of Ehrenreich (Ref. A-15) are also included: --- Weiss; ——— Ehrenreich; • this report.

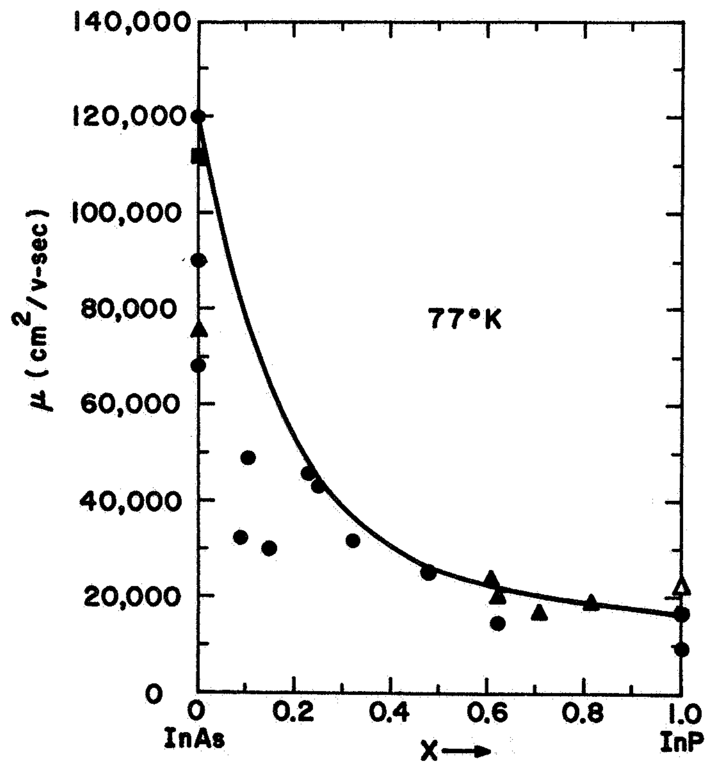

Figure A-5.

The dependence of the electron mobility on alloy composition in the system $InAs_{1-x}P_x$ at 77°K.

C. Doping. -- Doping of InAs has been investigated using H_2Se gas as a source of Se for n-type doping, and zinc for p-type doping. Electron concentrations as high as $3x10^{19}/cm^3$ were achieved and in general these crystals exhibit mobilities comparable to the best reported in the literature for untreated samples (Refs. A-18 - A-19). For example, at carrier concentrations of $1x10^{18}$ and $3x10^{19}$ cm^{-3} the mobility values at room temperature are 10,000 and 1,500 cm^2/V-sec, respectively. Thus, doping to these high donor concentrations does not degrade the material. With respect to hole concentrations, values in the range of $5x10^{17}$ to $7x10^{18}/cm^3$ can be readily obtained, with mobilities between 150 and 90 cm^2/V-sec for this doping range.

Both n- and p-type doping were also demonstrated for some $InAs_{1-x}P_x$ alloys, and for InP, as characterized by point-contact breakdown and thermal probe measurements. In addition, multilayer structures involving both n- and p-type regions were prepared for selected alloy compositions.

IV. Conclusions

The ability to prepare high-quality material by this growth method, which was previously demonstrated in the preparation of $GaAs_{1-x}P_x$ alloys, has now been extended to the preparation of $InAs_{1-x}P_x$ alloys. Electron mobilities have been obtained for these $InAs_{1-x}P_x$ alloys which are higher than previously reported. Both n- and p-type doping can be achieved over a broad resistivity range, and these doped layers can be incorporated in multilayer structures. Vegard's law of solid solutions was found to be obeyed in this alloy system.

V. Acknowledgments

The authors wish to express their appreciation to D. Richman for valuable suggestions and discussions, and to R. Paff for performing the x-ray analysis.

References

A-1. O. G. Folberth, Z. Naturforsch. 10a, 502 (1955).

A-2. H. Weiss, ibid. 11a, 430 (1956).

A-3. R. Bowers, et al., J. Appl. Phys. 30, 1050 (1959).

A-4. N. Holonyak, Jr., et al., Metallurgy of Semiconductor Materials, (Interscience Publishers, Inc., New York, 1962) p. 49.

A-5. S. Ku, J. Electrochem. Soc. 110, 991 (1963).

A-6. G. E. Gottlieb, ibid. 112, 192 (1965).

A-7. M. Rubenstein, ibid. 112, 426 (1965).

A-8. J. J. Tietjen and J. A. Amick, ibid. 113, 724 (1966).

A-9. J. J. Tietjen, et al., Trans. TMS-AIME 239, 385 (1967).

A-10. D. Richman and J. J. Tietjen, ibid. 239, 418 (1967).

A-11. C. J. Nuese, et al., ibid. 242, 400 (1968).

A-12. R. E. Enstrom and C. C. Peterson, ibid. 239, 413 (1967).

A-13. J. J. Tietjen, et al., Solid State Electronics 9, 1049 (1966).

A-14. W. Koster and W. Ulrich, Z. Metallk. 49, 365 (1958).

A-15. B. L. Goydish, to be published.

A-16. H. Ehrenreich, J. Phys. Chem. Solids 12, 97 (1959).

A-17. G. R. Cronin and S. R. Borello, J. Electrochem. Soc. 114, 1078 (1967).

A-18. T. C. Harman, et al., Phys. Rev. 104, 1562 (1956).

A-19. C. Hilsum and A. C. Rose-Innes, Semiconducting III-V Compounds, (Pergamon Press Ltd., London, 1961) p. 132.

APPENDIX B

Vapor-Phase Growth of Epitaxial $GaAs_{1-x}Sb_x$ Alloys Using Arsine and Stibine

R. B. Clough and J. J. Tietjen
RCA Laboratories, Princeton, New Jersey

ABSTRACT

A technique previously used to prepare alloys of $InAs_{1-x}P_x$ and $GaAs_{1-x}P_x$, using the gaseous hydrides arsine and phosphine, has been extended to grow single-crystalline $GaAs_{1-x}Sb_x$ by replacing the phosphine with stibine. Procedures were developed for handling and storing stibine which now make this chemical useful for vapor-phase growth. This represents the first time that this series of alloys has been grown from the vapor phase. Layers of p-type GaSb and GaSb-rich alloys have been grown with the carrier concentrations comparable to the lowest ever reported. In addition, a p-type alloy containing 4% GaSb exhibited a mobility of 400 $cm^2/V\text{-}sec$ which is equivalent to the highest reported for GaAs.

I. Introduction

Recently, interest has been shown in the preparation and properties of $GaAs_{1-x}Sb_x$ alloys, since it was predicted (Ref. B-1) that for compositions in the range of $0.1 < x < 0.5$, they might provide improved Gunn devices. However, preparation of these alloys presents fundamental difficulties. In the case of liquid-phase growth, the large concentration difference between the liquidus and solidus in the phase diagram, at any given temperature, introduces constitutional supercooling problems. It is likely that, for this reason, virtually no description of the preparation of $GaAs_{1-x}Sb_x$ by this technique has been reported. In the case of vapor-phase growth, problems are presented by the low vapor pressure of antimony and the low melting point of GaSb and many of these alloys. In previous attempts (Ref. B-1) at the vapor-phase growth of these materials, using antimony pentachloride as the source of antimony vapor, alloy compositions were limited to those containing less than about 2% GaSb. This was in part due to the difficulty of avoiding condensation of antimony on introducing it to the growth zone.

A growth technique has recently been described (Ref. B-2) for the preparation of III-V compounds in which the hydrides of arsenic and phosphorus (AsH_3 and PH_3) are used as the source of the group V element. With this method, $GaAs_{1-x}P_x$ and $InAs_{1-x}P_x$ have been prepared (Refs. B-2 and B-3) across both alloy series with excellent electrical properties. Since the use of stibine (SbH_3) affords the potential for effective introduction of antimony to the growth apparatus, in analogy with the other V hydrides, this growth method has been explored for the preparation of $GaAs_{1-x}Sb_x$ alloys. In addition to GaSb, these alloys have now been prepared with values of x as high as 0.8. In the case of GaSb, undoped p-type layers were grown with carrier concentrations

equivalent to the lowest reported in the literature. Thus, it has been demonstrated that, with this growth technique, all of the alloys in this series can be prepared.

II. Experimental Procedure

A. Growth Technique. -- The growth apparatus, shown schematically in Figure B-1, and procedure are virtually identical to that described (Ref. B-2) for the

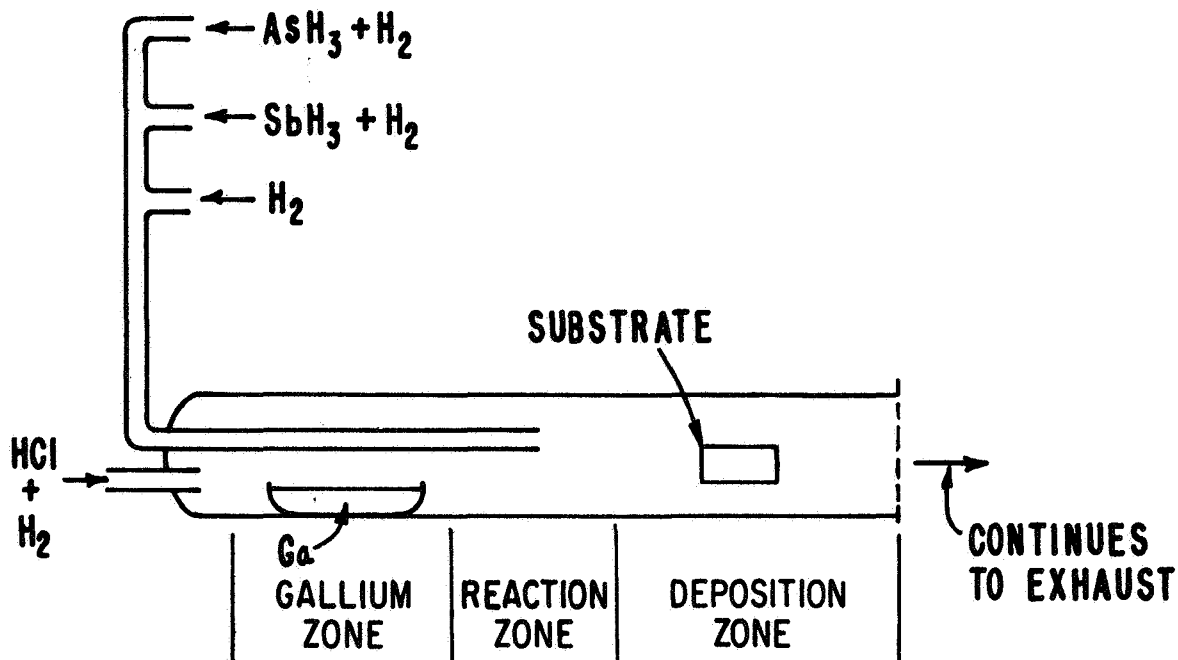

Figure B-1. Schematic representation of the vapor-deposition apparatus.

growth of $GaAs_{1-x}P_x$ alloys, with the exception that phosphine is replaced by stibine.* HCl is introduced over the gallium boat to transport the gallium predominantly via its subchloride to the reaction zone, where it reacts with arsenic and antimony on the substrate surface to form an alloy layer.

The fundamental limiting factors to the growth of $GaAs_{1-x}Sb_x$ alloys from the vapor phase are the low melting point of GaSb (712°C) and the low vapor pressure of antimony at this temperature (< 1 mm). Thus, relatively low antimony pressures must be employed, which, however, imply low growth rates. To provide low antimony pressures, very dilute concentrations of arsine and

* Purchased from Matheson Co., E. Rutherford, New Jersey.

stibine in a hydrogen carrier gas were used. Typical flow rates were about 4 cm^3/min of HCl, from 0.1 to 1 cm^3/min of AsH_3, and from 1 to 10 cm^3/min of SbH_3, with a total hydrogen carrier gas flow rate of about 6000 cm^3/min. The high linear velocities attendant with the high total flow rate delay cracking of the stibine until it reaches the reaction zone and prevent condensation of antimony in the system. To improve the growth rates, growth temperatures just below the alloy solidus are maintained to allow for a maximum partial pressure of antimony in the system. Typical temperatures used are gallium zone and reaction zone at 850°C, with the growth zone held at temperatures from 650 to 750°C.

Substrates of semi-insulating GaAs oriented 3° off the <100> axis were used in order to make electrical measurements, since the growth rates were too low to result in self-supporting epitaxial layers. As pointed out below, growth on these substrates has a deleterious effect on the electrical properties of the epitaxial layers.

B. Use of Stibine. -- Since little was known of the properties and handling procedures for stibine, experiments were performed to determine these. The vapor pressure was measured from -195°C to +27°C and found to agree with that obtained by Berka et al. (Ref. B-4) We found it to be more stable than anticipated, especially if stored in the dark. Although it was reported (Ref. B-5) that stibine has a half-life of from 2 to 4 hours at room temperature, we found that there was no measurable decomposition at 0°C for a period of 12 hrs. Thus, the gas can easily be kept above its boiling point (-18°C) for use during growth. We found it to be stable for a period of several months at -78°C (solid CO_2 temperature), so that it may be stored at this temperature prior to use.

Based on this stability data, a simple technique to use the stibine was established using the apparatus shown in Figure B-2. The stibine is stored at -78°C (solid CO_2 temperature) in the liquid state. For use during growth, an aliquot portion is first distilled from the storage cylinder to a reserve cylinder at -195°C (liquid-nitrogen temperature). The reserve cylinder is then warmed to 0°C and the distillation rate established by measuring the stibine pressure at this temperature. Typically, the distillation rates for our apparatus were about 0.01 mole/min. (They are very sensitive to slight temperature changes of the storage cylinder and, therefore, must be carefully monitored.) The stibine at 0°C is then pressurized with hydrogen for use during growth. To increase the amount of mixing, the hydrogen is introduced at high velocity. By preparing each aliquot immediately prior to use, problems due to settling of the mixture were minimized.

III. Results

Using this technique, we have grown alloys of $GaAs_{1-x}Sb_x$ with compositions ranging from 1 to 80 mole percent GaSb, as well as GaSb. This is the first time that they had been prepared from the vapor phase over this range of compositions. In a previous report (Ref. B-1) the preparation of $GaAs_{1-x}Sb_x$ was limited to 2 mole percent GaSb. These layers are all monocrystalline and epitaxial.

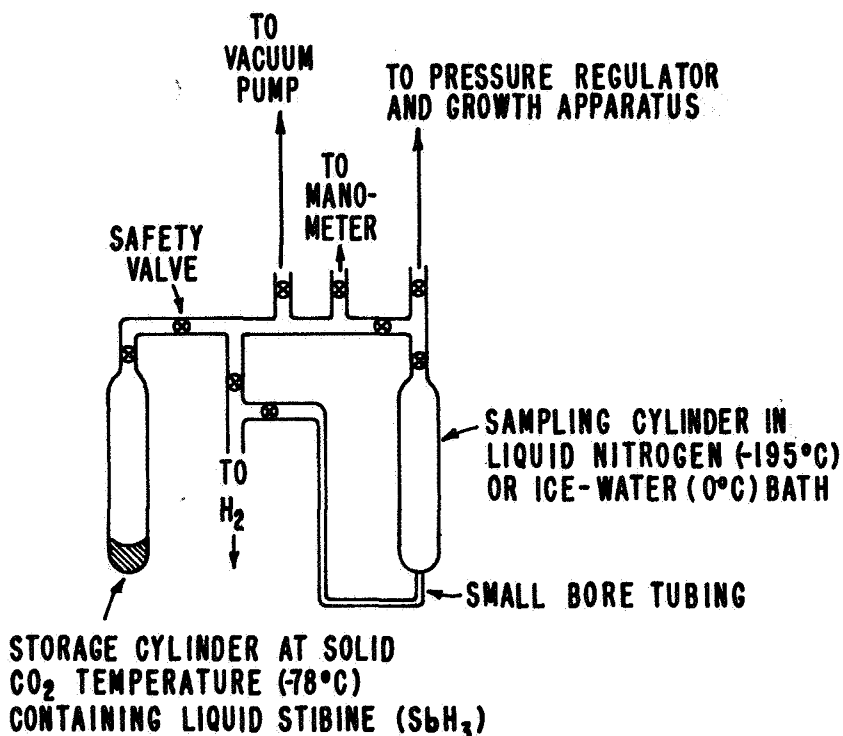

Figure B-2. Schematic representation of the stibine storage and sampling apparatus.

A. Growth Conditions. -- Studies on the effect of flow rates and growth temperature on the composition of the grown layers have shown the following. First, the mole fraction of antimony in the vapor phase is always greater than that in the grown layers. This indicates that there is a greater rate of incorporation of arsenic than antimony in the alloys, even though the vapor pressure of antimony is over four orders of magnitude lower than that of arsenic at the growth temperature. Second, the composition of the grown layers is independent of the growth temperature, varying less than $\pm$ 0.5 mole percent over approximately a 200°C range of growth temperature. Thus, the composition of the grown layers is a function only of the composition of the gas phase, so that all of the alloys in the series may be grown by selecting the appropriate flow rates of arsine and stibine.

B. Electrical Properties. -- The results of Hall coefficient and resistivity measurements for these alloys are presented in Table B-1. The carrier concentrations obtained for the p-type GaSb and GaSb-rich alloys are somewhat lower than those reported for melt-grown GaSb, where only a limited number of undoped p-type crystals have been grown with hole concentrations in the 10^{16} cm^{-3} range.

TABLE B-1

ELECTRICAL PROPERTIES OF P-TYPE $GaAs_{1-x}Sb_x$ ALLOYS

x	Hole Concentration (cm^{-3})		Hole Mobility (cm^2/V-sec)	
	300°K	77°K	300°K	77°K
0.01	$1.8x10^{15}$	$1.2x10^{15}$	220	400
0.02	$1.3x10^{16}$	$5.1x10^{15}$	190	700
0.04	$3.0x10^{15}$	--	400	--
0.10	$1.2x10^{18}$	$4.5x10^{17}$	55	160
0.21	$2.9x10^{17}$	$1.7x10^{17}$	45	80
0.31	$1.5x10^{18}$	$1.5x10^{18}$	24	30
0.62	$9.0x10^{18}$	$1.2x10^{19}$	20	15
0.70	$3.4x10^{16}$	--	251	--
0.75	$1.0x10^{17}$	--	48	--
0.80	$4.6x10^{16}$	--	21	--
1.00	$1.2x10^{19}$	$1.9x10^{19}$	215	120
1.00	$6.0x10^{16}$	$1.2x10^{16}$	240	270
1.00	$4.7x10^{16}$	--	120	--
1.00	$2.3x10^{17}$	$4.3x10^{16}$	336	405

One explanation for this is that the acceptor concentration is due to excess gallium on antimony sublattice sites (Ref. B-6) and is supported by the fact that the lowest hole concentrations reported (Ref. B-7 - B-8) were obtained only with an antimony-rich melt. In the case of vapor-phase growth of GaSb, the lower carrier concentrations obtained may be due to the excess antimony pressure in the growth zone.

Due to the thermodynamic reasons states previously, the growth rates of these alloys were generally low (< 5 microns/hr), so that in order for electrical measurements to be made, semi-insulating GaAs substrates were used. This has the detrimental effect of producing strain in the grown layers due to

a mismatch in lattice constant and thermal expansion coefficient between the substrate and grown layer. As a result, the GaSb-rich compounds, which are all p-type, generally exhibit low mobilities compared with melt-grown GaSb, where hole mobilities are typically 700-800 cm^2/V-sec. It is expected that compositional grading, or deposition on GaSb substrates, would result in higher mobilities. In this respect, it is noteworthy that the hole mobility of 400 cm^2/V-sec achieved in an alloy containing only 4 mole percent GaSb is equivalent to the highest value ever reported for unalloyed GaAs. A few layers, all less than 3 mole percent GaSb, were n-type, and these show (Table B-2)

TABLE B-2

ELECTRICAL PROPERTIES OF N-TYPE $GaAs_{1-x}Sb_x$ ALLOYS

x	Net Carrier Conc., cm^{-3}		Electron Mobility cm^2/V-sec	
	at 300°K	at 77°K	at 300°K	at 77°K
< 0.01	1.1×10^{16}	7.8×10^{15}	3840	4975
0.025	4.5×10^{16}	2.6×10^{16}	2920	5550
0.033	4.7×10^{16}	--	5370	--

electron mobilities which, in general, are slightly lower than commonly observed for melt-grown n-type GaAs. Those p-type alloys having extremely low mobility show very broad x-ray diffraction peaks with half-widths often an order of magnitude wider than those of the substrate diffraction peak, indicating either considerable inhomogeneous strain in the layers or an inhomogeneous composition.

IV. Conclusions

Stibine can be successfully used as a source of antimony in vapor-phase crystal growth, and $GaAs_{1-x}Sb_x$ alloys can be prepared from the vapor phase across the entire alloy series. This growth technique shows promise of preparing these alloys with good electrical properties if problems of strain and inhomogeneity can be overcome.

VI. Acknowledgments

The authors gratefully acknowledge the assistance of T. V. Pruss in the growth of these alloys, R. J. Paff and R. T. Smith for x-ray analysis, and D. Richman for many valuable suggestions.

References

B-1. G. F. Day, New Gunn Effect Materials, Varian Associates, Technical Report AFAL-TR-67-2, March 1967, Contract No. AF33(615)-1988.

B-2. J. J. Tietjen and J. A. Amick, J. Electrochem. Soc. 113, 724 (1966).

B-3. J. J. Tietjen, H. P. Maruska, and R. B. Clough, to be published.

B-4. L. Berka, T. Briggs, M. Millard, and W. Jolly, J. Inorg. Nucl. Chem. 14, 190 (1959).

B-5. K. Tamaru, J. Phys. Chem. 59, 1084 (1955).

B-6. R. K. Willardson, Annals of the New York Academy of Sciences 137, 49 (1966).

B-7. D. Effer and P. J. Etter, J. Phys. Chem. Solids 25, p. 451 (1964).

B-8. R. D. Baxter, F. J. Reid, and R. T. Bate, Bull. Am. Phys. Soc. 9, 646 (1964).

DISTRIBUTION LIST CONTRACT NAS 12-538

U. S. Army Electronics Command
Fort Monmouth, New Jersey
07703
Attn:Mr. Arthur Boatright

National Aeronautics & Space
Administration
Attn: US/W.M.Morgan
Sci. & Tech. Info. Div.
Washington, D.C. 20546 2 +

National Aeronautics & Space
Administration
Attn: Office of Technology
Utiliztion
Washington, D.C. 20546

National Aeronautics & Space
Administration
Atn: REE/C. E. Pontious
Washington, D.C. 20546

National Aeronautics & Space
Administration
Attn: R/Dr. W. C. Dunlap
Electronics Res. Center
Cambridge, Massachusetts 02139

National Aeronautics & Space
Administration
Attn: RM/Dr. D. Warschauer
575 Technology Square
Washington, Mass 02139

National Aeronautics & Space
Administration
Attn: RR/Dr. H. Roth
575 Technology Square
Cambridge, Mass 02139

National Aeronautics and Space
Administration
Attn: Technology Utilization
575 Technology Square
Cambridge, Mass 02139

Mr. John K. Kennedy
AFCRL, Stop 30
L. G. Hanscom Field
Bedford, Mass 01731

Dr. L. Wandinger
USA Electronics Command Lab.
Solid State & Fre. Cont. Div.
Fort Monmouth, New Jersey
07703

Dr. Michael Amsterdam
Micro-Space Electronics
152 Floral Ave.
Murray Hill, N. J.

Dr. M. Rubenstein
Westinghouse Elec. Corp.
Res. & Dev. Center
Pittsburgh, Penna 15235

Dr. S. F. Snow
Tyco Labs., Inc.
Bear Hill
Waltham, Mass 02154

Mr. Paul E. Greene
Hewlett Packard
1501 Page Mill Rd.
Palo Alto, California 94304

Mr. Bruce Cairns
Fairchild Semiconductor R&D
Laboratory
4001 Junipero Serra Blvd.
Palo Alto, California 94304

Mrs. Palma Marton
Tech. Librarian
Electro-Optical Systems, Inc
300 N. Halstead St.
Pasadena, California 91107

Dr. Brian Fitzpatrick
Solid State Chemistry
Ion Physics Corp.
P. O. Box 98
Burlington, Mass 01803

Dr. F. L. Morritz
Autonetics
3370 East Anaheim Rd.
Anaheim, California

Mr. Joseph Wenckus
Arthur D. Little, Inc.
Acorn Park
Cambridge, Mass

Dr. Gunther A. Wolff
Tyco Laboratories, Inc.
Bear Hill
Waltham, Mass 02154

Mr. M. Braunstein
Highes Research Laboratories
Malibu, California 90265

Dr. Joseph E. Johnson
Wstinghouse Res. Labs
Beulah Road,Churchillboro
Pittsburgh, Penna 15235

Dr. Alex Noreika
Westinghouse Res. Labs
BeulahRoad, Churchill boro
Pittsburgh, Penna 15235

Dr. G. K. Wehner
Litton Systems, Inc.
Applied Science Div.
Minneapolis, Minn 55413

Dr. Wm. J. Moroney
Director of Semiconductor Dev.
Microwave Associates, Inc.
Burlington, Mass 01803

Dr. E H. Blevis
The Marquardt Corp
Van Nys, California

Dr. Alan Strauss
M.I.T. - Lincoln Laboratories
Lexington, Mass

Dr. Harry C. Gatos
Dept. of Elect. Eng.
M.I.T.
Cambridge, Mass

Dr. Robert H. Rediker
Dept. of Elect. Eng.
M.I.T.
Cambridge, Mass

Dr. J. R. Biard
Texas Instruments
Dallas, Texas

Dr. D. V. Geppert
Stanford Research Inst.
Menlo Park, California

Dr. Julian A. Crawford
Systems Res. Labs.
Dayton, Ohio 45432

Dr. James J. Casey
Sprague Electric Co.
No. Adams, Mass

Dr. T. Harmon
M.I.T. - Lincoln Laboratories
Lexington, Mass

Dr. Hnery T. Minden
Sperry Rand Tes. Center
Sudbury, Mass 01776

Dr. Robert N. Hall
General Elec. R&D Center
Schenectady, New York 12301

Dr. A. C. Beer
Battelle Memorial Inst.
Columbus, Ohio

A. F. Materials Lab.
Attn: Elizabeth H. Tarrants
Wright-Patterson AFB, Ohio
45433

Dr. Marshall Nathan
International Bus. Machines
Corporation
Yorktown Heights, New York

Dr. Egon E. Loebner
Hewlett-Packard Labs.
1501 Page Mill Rd.
Palo Alto, California 94304

Dr. Robert A. Laudise
Bell Telephone Labs.
Murray Hill, N. J.

Dr. Forest Williams
Monsanto
St. Louis, Mo.

Dr. James R. Henderson
Chief, Solid State Physics
McDonnel Sec.-Doulgals Aircraft
San Bernardino, California
92410

Dr. Ting L. Chu
Southern Methodist University
Electronic Sciences Center
Dallas, Texas 75222

Arthur R. Clawson
Naval Weapons Center
Corona Labs. - Code C613
Corona, California 91720

Richard Cornelissen
Air Force Cambridge Res. Labs.
L. G. Hanscom Field
Bedford, Mass

K. M. Hergenrother
Northeastern University
Room 333-DA
360 Huntington Ave.
Boston, Mass 02115

Dr. Gerald Pearson
Stanford University
Electronics Labs.
Stanford, California 94305

F. J. Reid
General Telephone & Electronics
Labs.
208-20 Willets Pt. Blvd.
Bayside, New York 11360

D. W. Shaw
Texas Instuments, Inc.
P. O. Box 5936 M.S. 145
Dallas, Texas 75222

Dr. Raymond Solomon
Fairchild Semiconductor R&D
4001 Miranda Ave
Palo Alto, California 94304

Dr. William G. Spitzer
Univ. of Southern California
Vivian Hall of Engineering
Los Angeles, California 90004

Hans Strack
Texas Instruments, Inc
P. O. Box 5012, M.S. 86
Dallas, Texas 75222

Charles M. Wolfe
M.I.T. Lincoln Laboratory
Lexington, Mass 02173